2006

Intraoperative solid-state based urethral dosimetry in low dose rate prostate brachytherapy

Dean Cutajar
University of Wollongong, deanc@uow.edu.au

G. J. Takacs
University of Wollongong, gjt@uow.edu.au

M. L. Lerch
University of Wollongong, mlerch@uow.edu.au

T. Braddock
University of Wollongong, braddock@uow.edu.au

J. A. Bucci
St George Cancer Care Centre, Australia

See next page for additional authors

Authors

Dean Cutajar, G. J. Takacs, M. L. Lerch, T. Braddock, J. A. Bucci, J. Brady, L. J. Duggan, K. E. Enari, M. Zaider, M. Zelefsky, and Anatoly B. Rosenfeld

Intraoperative Solid-State Based Urethral Dosimetry in Low Dose Rate Prostate Brachytherapy

D. L. Cutajar, *Member, IEEE*, G. J. Takacs, M. L. F. Lerch, *Member, IEEE*, T. Braddock, J. A. Bucci, J. Brady, L. J. Duggan, K. E. Enari, M. Zaider, M. Zelefsky, and A. B. Rosenfeld, *Senior Member, IEEE*

***Abstract*—This paper presents in phantom testing of a recently developed intraoperative minidosimetry system, designed to measure the dose along the urethra during low dose rate prostate brachytherapy. This system is based on a silicon minidetector and uses spectroscopy to calculate the localized dose from the treatment radiation. The minidosimetry system was demonstrated to be operational at body temperature, with a near isotropic response to radiation at all angles. Phantom measurements have shown the minidosimetry system to measure the dose from multiple seeds to within 5% of planning system calculated doses. This system is an ideal complement to ultrasound guided seed placement in providing online direct dosimetry during seed implantation, as well as providing dose planning system verification through post implant dosimetry.**

***Index Terms*—Brachytherapy, dosimetry, spectroscopy.**

I. Introduction

LOW dose rate brachytherapy through transperineal placement of ^{125}I and ^{103}Pd based seeds is a common treatment modality for early stage prostate cancer [1]. The precision of transrectal ultrasound guided localization of the guiding needles, as well as an increase in the sophistication of computerized treatment planning has lead to an increase in the popularity of this modality [2]. Quality assurance is performed postimplant through dosimetric evaluations, where the source placement relative to the prostate is obtained, using CT to identify the seed positions [3].

Medical complications, specifically acute urinary side effects [4], can arise from interstitial prostate brachytherapy due to errors in seed placement. Several factors may lead to the misplacement of seeds throughout the treatment. During implantation, the guiding needles may diverge as various layers of tissue are penetrated [5], depositing seeds in an incorrect location; the seeds may drift out of position due to blood flow; oedema may alter the size and shape of the prostate; and gland motion may occur during treatment [6]. Any combination of these factors may lead to the urethral dose escalating above planned levels. Wallner *et al.* [7] observed an increase in grade-3 late urethral toxicity for urethral doses exceeding 400 Gy. There is a need to monitor the urethral dose during implantation to manage urethral toxicity, as well as post implant to verify dose planning. The American Brachytherapy Society (ABS) has requested the urethral dose be recorded for correlation with urethral toxicity [8], recommending the doses be obtained at the center of the urethra, in half centimeter intervals, measured from the base of the prostate to the apex. The maximum and mean doses along the urethra should be specified [8].

We have developed an *in vivo* minidosimetry system which may be placed within a Foley catheter for dose measurements along the urethra, both intraoperative and postimplant. This system uses a silicon minidetector with an active volume of less than 1 mm^3, operating in spectroscopy mode, connected to a data acquisition system that calculates the dose rate using "spectroscopic dosimetry." Brachytherapy seeds contain radioactive sources, usually ^{125}I or ^{103}Pd. These radioactive sources emit low energy photons with a distinct energy spectrum, at very low dose rates, that are impossible to measure with conventional detectors in confined spaces. Conventional methods of radiation detection with diodes involve measuring the induced current with an electrometer. The low dose rates (1–5 cGy/hr) will only induce current to the order of 0.1 ρ A. At these low energies, approximately 27 keV for ^{125}I based seeds, most energy loss for photons in water/tissue occurs through the photoelectric effect. The Compton scattering cross-section is significant, but energy loss due to the Compton effect is minimal. The photon peaks will be attenuated in intensity. The number of counts in the photopeaks of a measured spectrum can be related to the dose rate at the point of measurement. The complexity of the dosimetry of ^{125}I and ^{103}Pd seeds is due to the low dose rates, anisotropy of dose about the seeds, and rapidly diminishing dose with distance from the seed. Spectroscopic dosimetry does not require tissue equivalency of the detector and is very sensitive as it is based on the registration of single photons. Theoretical aspects and Monte Carlo simulations justifying the proposed method can be found in Rosenfeld *et al.* [9].

In order for this system to be viable, the minidetector needs to have an isotropic response to radiation from all angles and needs to produce results in agreement with doses determined by conventional CT and ultrasound based dose planning systems. Several in phantom measurements were performed to test the detector response at various dose rates and the detector isotropy. These measurements were compared to predicted doses, generated using VariSeed 7 dose planning software from Varian Medical Systems, Palo Alto, CA. This software uses point source approximations to accurately predict dose distributions for treat-

Manuscript received November 15, 2004.

D. L. Cutajar, G. J. Takacs, M. L. F. Lerch, T. Braddock, J. Brady, and A. B. Rosenfeld are with the Centre for Medical Radiation Physics, University of Wollongong, Wollongong, NSW, Australia, 2522.

J. A. Bucci, L. J. Duggan, and K. E. Enari are with the St. George Cancer Care Centre, St. George Hospital, Kogarah, NSW, Australia, 2217.

M. Zaider and M. Zelefsky are with the Memorial Sloan Kettering Cancer Center, New York, NY 10021 USA.

Digital Object Identifier 10.1109/TNS.2006.873003

ments involving a large number of seeds. Dose distribution calculations involving a small number of seeds require the seed dose rate anisotropy to be taken into account. Anisotropy corrections, generated using Monte Carlo simulations and confirmed using the TG43 protocol [10], were applied to the VariSeed 7 predicted doses for the comparison with the minidosimeter measured doses.

II. Materials and Methods

The urethra minidosimetry probe was constructed using a silicon minidetector inside the tip of a rubber tube of length 30 cm and diameter 3 mm, connected to a charge sensitive preamplifier at the opposite end of the tube. The minidetector was constructed from 10 kΩ high resistivity silicon, with a cross section of 0.8×2.5 mm and a depletion region of 300 μm depth. The minidetector was designed by the Centre for Medical Radiation Physics and manufactured at SPO-BIT, Kiev, Ukraine. The design featured an optimized geometry and packaging to allow for an isotropic response to radiation from all angles and to provide X-ray spectroscopy at 38 °C (to allow for *in vivo* measurements). The preamplifier output was connected to a data acquisition system consisting of a shaping amplifier, adjustable lower voltage pulse height discriminator, pulse counter, microprocessor, and LCD display. The pulse height discriminator is used to set a cutoff between pulses due to photon peaks and lower level noise, as well as serving as an adjustment for fine dose rate calibration. Pulses with amplitudes above the discriminator level are sent to the microprocessor for further processing and determination of the dose rate and extrapolated total delivered dose in tissue. The microprocessor uses a precalibrated algorithm to calculate the measured dose rate from the number of counted pulses and the acquisition time. The current dose rate and expected total dose after full decay are shown on the LCD display. The minidosimetry system also contains an analogue output from the shaping amplifier to allow connectivity to an external system, such as an MCA for calibration and quality assurance testing, or a dose planning system for intraoperative planning.

A. Calibration

A ^{125}I based brachytherapy seed, no. 6711 from Amersham Health, Inc., Princeton, NJ, was placed in a Perspex phantom, 1 cm from the minidosimeter detector. The detector was in line with the transverse axis of the seed. The expected dose rate was calculated using the formula [11]

$$D_r = \frac{\Lambda S_k g(r)}{r^2} \quad (1)$$

where S_k is the seed air kerma strength and Λ the specific dose rate (dose rate in a water per air kerma strength, 1 cm from the seed on the transverse axis), $g(r)$ is the radial dose function, and r is the radial distance from the point of measurement to the seed

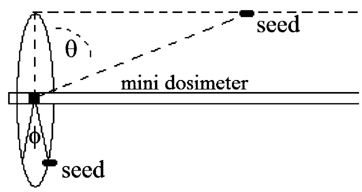

Fig. 1. Azimuthal isotropy measurement geometry (solid lines) and polar angle measurement geometry (dotted lines), where ϕ is the azimuthal angle about the minidosimeter axis and θ is the polar angle. The horizontal dotted line represents the location of the catheter within which the seed position was varied for the polar angle measurements.

center. At 1 cm from the seed on the transverse axis, $g(r) = 1$, (1) becomes

$$D_r = \Lambda S_k. \quad (2)$$

The updated Task Group No. 43 report [10] lists the dose rate constant, Λ, as 0.965 cGyh^{-1}mCi^{-1}, for 6711 seeds with source strength specified in terms of apparent activity (A_{app}) instead of air kerma. Thus, the dose rate may be calculated using the formula

$$D_r = \Lambda A_{\mathrm{app}}. \quad (3)$$

The dose rate algorithm on the minidosimetry system was then adjusted to output the expected dose rate in water for this seed measurement.

B. Azimuthal Isotropy Measurements

The isotropy of the response of the detector about the minidosimeter axis was measured. The minidosimeter probe was placed in a Perspex phantom, 1 cm from a 6711 seed, on the transverse axis of the seed. The seed position was rotated about the axis of the minidosimeter with the dose recorded every 30°, as shown by Fig. 1.

C. Polar Isotropy Measurements

A gel phantom was constructed to measure the dose rates of seeds in a 3-D geometry. The phantom contained a straight artificial urethra for which to place the dosimeter, and allowed catheters (ProGuide Sharp Needles from Nucletron, Veenendaal, Utrecht, The Netherlands [14]) to be inserted parallel to the urethra, with which seeds could be placed in desired locations within the phantom. The phantom was filled with a water based gel.

A catheter was placed in the phantom, 0.5 cm from the artificial urethra. The total dose expected in a fixed location of the urethra was measured for a 6711 seed placed in several locations along the catheter, with each location subtending a different polar angle about the minidosimeter detector and seed, as shown in Fig. 1. The measured expected total doses were compared to the total doses calculated using VariSeed 7, a treatment planning system from Varian Medical Systems .

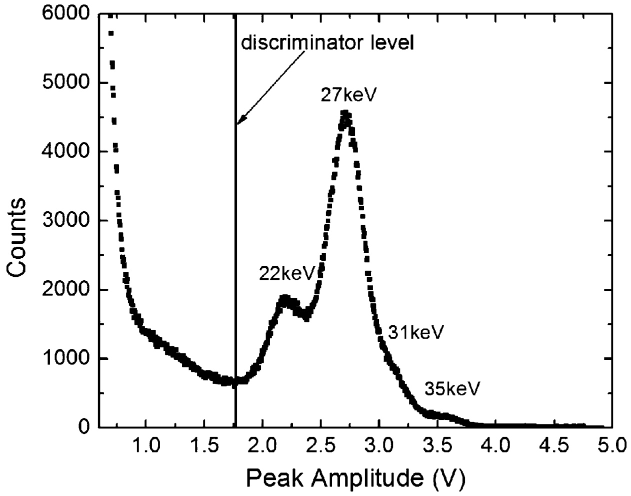

Fig. 2. Spectrum of a model 6711 seed in Perspex, 1 cm from the minidosimeter detector. The discriminator level was set at the local minimum below the photopeaks of the spectrum, approximately 19 keV. Low level noise and an offset in the MCA restricted the measurements to pulses greater than 0.5 V amplitude.

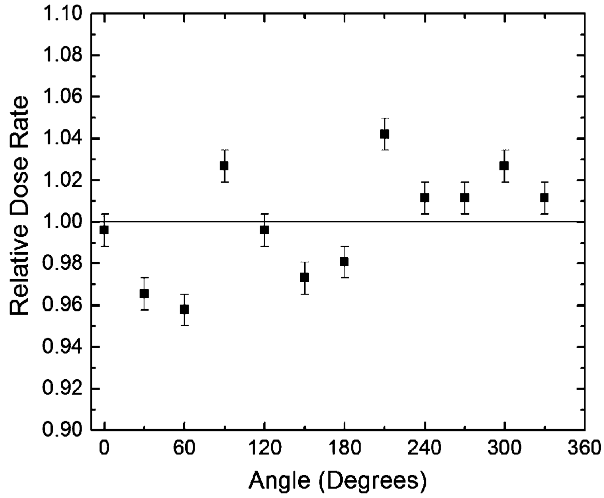

Fig. 3. Relative dose rate versus Azimuthal angle.

D. Depth–Dose Measurements

The total expected dose was measured in the urethra for a 6711 seed in the gel phantom, for various distances between the seed and the minidosimeter detector, with the detector on the transverse axis of the seed ($\theta = 0^\circ$). The decay-corrected activity of the seed was calculated to be 0.351 mCi at the time of measurement. These doses were compared to the total doses calculated using VariSeed 7.

E. Multiple Seed Measurements

There were 12 seeds, each one model 6711, placed in the gel phantom about the urethra containing the minidosimeter detector. The decay-corrected activity of each of the seeds was calculated to be 0.351 mCi at the time of measurement. The activity was assumed to be the same for all seeds as this is acceptable in practice for seeds from the same batch. The physical characteristics (size, source distribution) were also assumed to be identical. Four seeds were placed in the same vertical plane as the detector, in catheters 0.5 cm, 1 cm, 1 cm, and 1.41 cm from the urethra, running parallel to the urethra. Four seeds were placed in the above catheters on a vertical plane 1 cm forward of the detector, and four seeds were placed in the above catheters on a vertical plane 1 cm beyond the detector. The total expected dose was measured using the urethral minidosimetry system. The measured dose was compared to the dose calculated using VariSeed 7.

III. Results

A. Calibration

Fig. 2 shows the energy spectrum from the calibration measurement, recorded on an MCA connected to the shaping amplifier analogue output. The lower level discriminator was set to 1.77 V, allowing only pulses with amplitudes above this to be counted by the system. The apparent activity of the seed was calculated to be 0.157 mCi, based on the initial activity and elapsed time. From (3), the expected dose rate was calculated to be 0.17 cGyh^{-1}. The dose rate algorithm on the minidosimetry system was adjusted to display an output of 0.17 cGyh^{-1} for the current measurement. Additionally, fine adjustments may also be made are also possible with discriminator level changing.

B. Azimuth Isotropy Measurements

Fig. 3 shows the relative dose rate, which is the measured dose rate normalized to the average, as measured with the minidosimetry system, of a 6711 seed located 1 cm from the minidosimeter detector, at various angles about the azimuth of the minidosimeter probe axis. The minidosimetry system shows an isotropic response to radiation from all azimuthal angles within $\pm 5\%$. The discrepancies may be due to the minidetector not being centered inside the probe, as well as a nonuniform detector packaging. The zero degree point was arbitrarily chosen as the detector packaging restricted the determination of the detector orientation.

C. Polar Isotropy Measurements

The expected total dose from a single seed, at multiple polar angles to the minidosimeter detector was plotted in Fig. 4 for both planned and measured doses. The results do not correlate for doses measured at polar angles 60° and above.

These discrepancies can be seen clearly in Fig. 5, where the difference between the doses measured with the minidosimetry system and the VariSeed 7 planned doses, as a percentage, was plotted against polar angle. Point source approximations were used by the planning software to calculate the expected doses. When calculating doses from brachytherapy seeds, seed geometry, and anisotropy should be taken into account [12].

A Monte Carlo simulation was performed using EGSnrc V4 [13]. DOSRZnrc was the code used to simulate the dose in cylindrical geometry of a 6711 seed in liquid water. The geometry of the seed, as shown in Fig. 6, was modeled on the dimensions used in simulations by Williamson [14].

The results from the simulation were used to generate anisotropy corrections for the VariSeed 7 planned doses. The Task Group No. 43 protocol [11] was used to confirm the

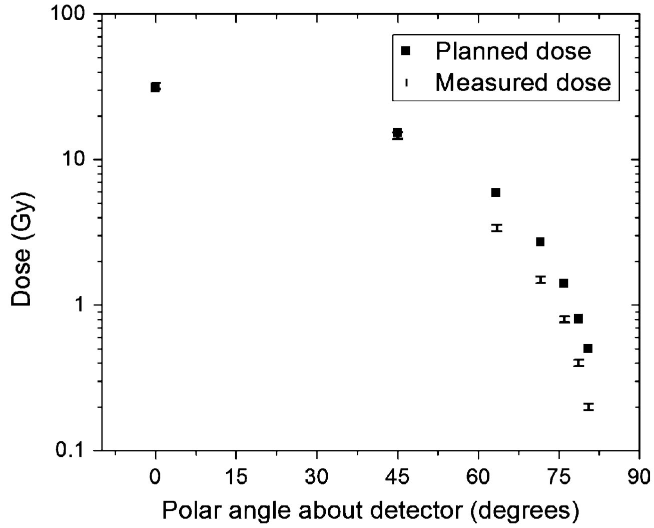

Fig. 4. Expected total dose versus polar angle of measurement for both planned and experimentally measured doses.

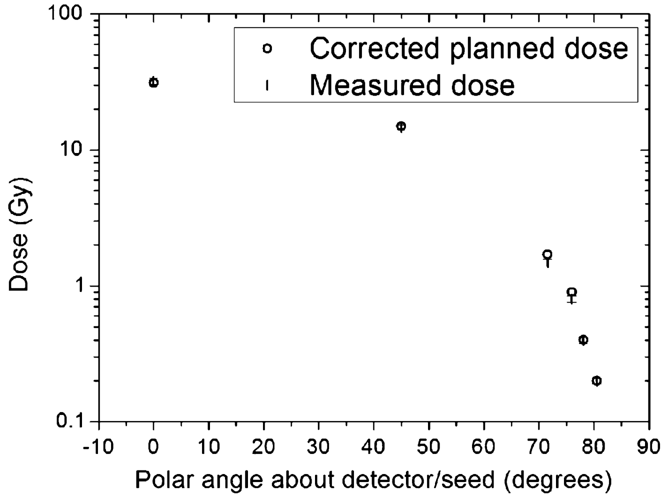

Fig. 7. Expected total dose versus polar angle for the measured and anisotropy corrected planned doses.

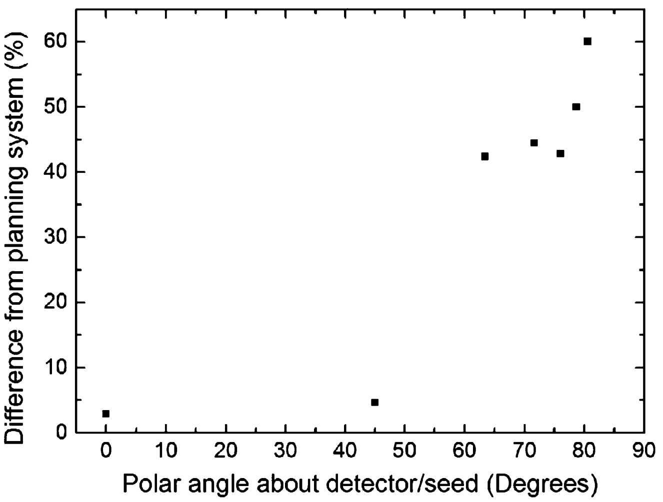

Fig. 5. The difference between the experimentally measured and the planned doses as a percentage versus polar angle of measurement.

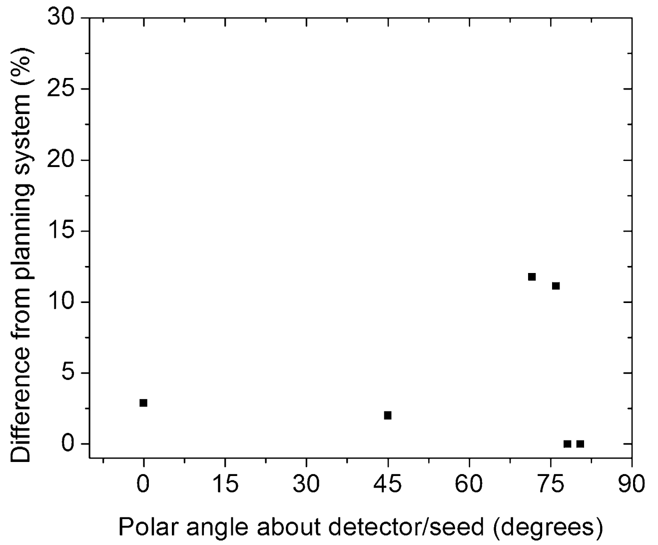

Fig. 8. The difference between the experimentally measured and the anisotropy corrected planned doses as a percentage versus polar angle of measurement.n

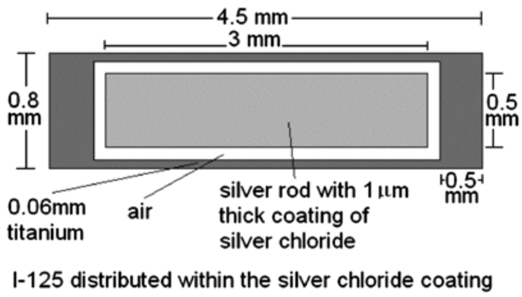

Fig. 6 Model 6711 seed geometry.

anisotropy corrections that were applied to the planned doses. The measured doses were plotted with the anisotropy corrected planned doses versus the polar angle in Fig. 7. The difference between the experimentally measured and the anisotropy corrected planned doses as a percentage versus polar angle of measurement was plotted in Fig. 8.

After anisotropy correction of the planned doses, the measured and planned doses have a greater correlation. The discrepancies that still remain may be due to errors in seed placement. The difficulty in positioning the seeds within the phantom introduced errors in seed localization. The dose decreases rapidly with distance from the source for low energy photons in water. Small errors in seed to detector distance can result in large errors in measured dose.

D. *Depth–Dose Measurements*

Depth–dose measurements were obtained for seeds on the transverse axis of the minidosimeter detector ($\theta = 0$) and plotted with the VariSeed 7 planned doses in Fig. 9.

The measured doses correspond to the planned doses within the errors of measurement, including the statistic of counts during the acquisition time of 10 seconds for seeds placed up to 2 cm from the minidosimeter detector.

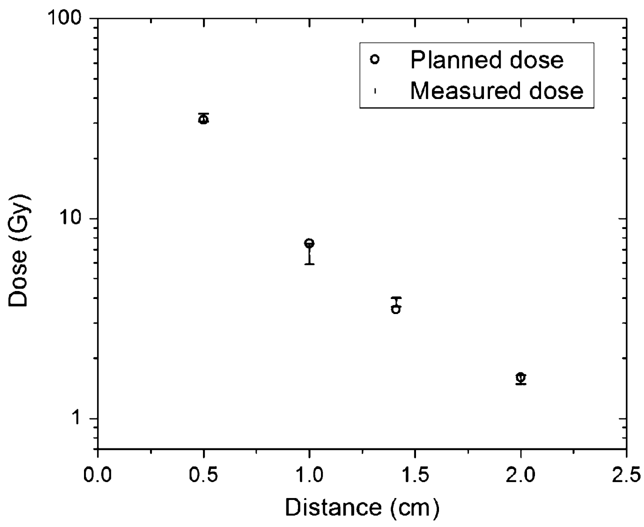

Fig. 9. Expected total dose versus distance for measured and VariSeed 7 planned doses.

E. Multiple Seed Measurements

The VariSeed 7 planned dose for the 12-seed configuration was 79.8 Gy at the point of minidetector of urethral probe in a phantom. After applying anisotropy corrections for the eight seeds that were in a different plane to the minidosimeter detector, the corrected planned dose was 73 Gy. The measured expected total dose was 70 Gy $\pm$ 3.5 Gy. The measured dose is within 5% of the planned dose for multiple seed measurements with anisotropy corrections for the dose planning software.

IV. Conclusion

The minidosimetry system has been shown to measure doses from ^{125}I based low dose rate brachytherapy seeds to an accuracy within 5% of the expected doses for seeds in a 3-D geometry about the minidosimeter detector, for 0.5 cm to 2 cm distances. Multiple seed measurements were also accurate to within 5% of planned doses. Discrepancies in the results may be attributable to errors in the seed-minidetector localization accuracy during the experimental phantom measurements. Localized doses in brachytherapy are very sensitive to seed position for seeds within centimeters of the point of measurement due to the short range of low energy photons in tissue and seed anisotropy.

The minidosimetry system contains a silicon minidetector inside a flexible plastic tube, small enough to be placed inside a Foley catheter for dose measurements along the urethra. The minidosimetry system may also be adapted to measure the dose to the rectum wall during low dose rate prostate brachytherapy.

This probe clearly demonstrates the advantage of *in vivo* urethral dosimetry. While dose planning systems are accurate for dose prediction along the transverse axis of seeds it is quite essential that anisotropy is accounted for at large polar angles. This is because most dose planning systems approximate seeds as point sources. This philosophy is not due to a lack of understanding but due to the impossibility of prediction of the polar angle (θ) for particular positions in the prostate when seeds have been dropped. In case of large distances between seeds and the point of consideration in the urethra, this error in total dose contribution at this point is negligible, however, in the case of seeds dropped close to the point of interest in the urethra (less then 0.5 cm) according to the plan, twisting of the seeds can produce large errors between the planned and real dose.

The minidosimetry system is suitable for intraoperative and postimplant measurements. The system will complement current systems in that the dose profile along the urethra will be available to practitioners during the procedure. If the dose to the urethra is exceeding tolerable limits, changes to the plan may be made in compensation. Postimplant measurements of the urethral dose profile will allow quality assurance of the implant as well as verification of the plan.

References

[1] R. E. Peschel, Z. Chen, K. Roberts, and R. Nath, "Long-term complications with prostate implants: Iodine-125 vs. Palladium-103," *Radiat. Oncol. Investig.*, vol. 7, pp. 278–288, 1999.

[2] G. S. Merrick, W. M. Butler, A. T. Dorsey, and H. L. Walbert, "Influence of timing on the dosimetric analysis of transperineal ultrasound-guided, prostatic conformal brachytherapy," *Radiat. Oncol. Investig.*, vol. 6, pp. 182–190, 1998.

[3] P. L. Roberson, V. Narayana, D. L. McShan, R. J. Winfield, and P. W. McLaughlin, "Source placement error for permanent implant of the prostate," *Med. Phys.*, vol. 24b, no. 2, pp. 251–257, Feb. 1997.

[4] D. Y. Gelblum, L. Potters, R. Ashley, R. Waldbaum, X. Wang, and S. Leibel, "Urinary morbidity following ultrasound-guided transperineal prostate seed implantation," *Int. J. Radiat. Oncol., Biol., Phys.*, vol. 45, pp. 59–67, 1999.

[5] S. Nath, Z. Chen, N. Yue, S. Trumpore, and R. Peschel, "Dosimetric effects of needle divergence in prostate seed implant using 125-I and 103-Pd radioactive seeds," *Med. Phys.*, vol. 27, no. 5, pp. 1058–1066, 2000.

[6] R. Taschereau, J. Roy, and J. Pouliot, "Monte Carlo simulations of prostate implants to improve dosimetry and compare planning methods," *Med. Phys.*, vol. 26, no. 9, pp. 1952–1959, 1999.

[7] K. Wallner, J. Roy, and L. Harrison, "Dosimetry guidelines to minimize urethral and rectal morbidity following transperineal I-125 prostate brachytherapy," *Int. J. Radiat. Oncol., Biol., Phys.*, vol. 32, pp. 465–471, 1995.

[8] S. Nag, R. J. Ellis, G. S. Merrick, R. Bahnson, K. Walner, and R. Stock, "American brachytherapy society (ABS) recommendations for reporting morbidity after prostate brachytherapy," *Int. J. Radiat. Oncol., Biol., Phys.*, vol. 54, no. N2, pp. 462–470, 2002.

[9] A. B. Rosenfeld and D. L. Cutajar, "In vivo dosimetry and seed localization in prostate brachytherapy with permanent implants," *IEEE Trans. Nucl. Sci.*, vol. 51, no. 6, pp. 3013–3018, Dec. 2004.

[10] M. J. Rivard, B. M. Coursey, L. A. DeWerd, W. F. Hanson, M. S. Huq, G. S. Ibbott, M. G. Mitch, R. Nath, and J. F. Williamson, "Update of AAPM Task Group No. 43 Report: A revised AAPM protocol for brachytherapy dose calculations," *Med. Phys.*, vol. 31, no. 3, pp. 633–674, Mar. 2004.

[11] R. Nath, A. S. Meigooni, and J. A. Meli, "Dosimetry on transverse axis of ^{125}I and ^{192}Ir interstitial brachytherapy sources," *Med. Phys.*, vol. 17, no. 6, pp. 1032–1040, Nov./Dec. 1990.

[12] R. Nath, L. L. Anderson, G. Luxton, K. A. Weaver, J. F. Williamson, and A. S. Meigooni, "Dosimetry of interstitial brachytherapy sources: Recommendations of the AAPM Radiation Therapy Committee Task Group No. 43," *Med. Phys.*, vol. 22, no. 2, pp. 209–234, Feb. 1995.

[13] I. Kawrakow and D. W. O. Rogers, "The EGSnrc Code System," NRC, Ottawa, ON, Canada, NRC Rep. PIRS-701, 2000.

[14] J. F. Williamson, "Monte Carlo evaluation of specific dose constants in water for I-125 seeds," *Med. Phys.*, vol. 15, no. 5, pp. 686–694, 1988.